GELF: A Global Error-based Learning Function for Globally Optimal Adaptive Reliability Analysis

Chi Zhang[1], Chaolin Song[1,2], Abdollah Shafieezadeh[1]
[1] Risk Assessment and Management of Structural and Infrastructure Systems (RAMSIS) Lab, Department of Civil, Environmental, and Geodetic Engineering, The Ohio State University, Columbus, OH, 43210, United States
[2] Department of Bridge Engineering, Tongji University, Shanghai, 200092, China

ABSTRACT

Kriging has gained significant attention for reliability analysis primarily because of the analytical form of its uncertainty information, which facilitates adaptive training and establishing stopping criteria for the training process. Learning functions play a significant role in both selection of training points and stoppage of the training. For these functions, most existing learning functions evaluate candidate training points individually. However, lack of consideration for the global effects can lead to suboptimal training. In addition, the subjectivity of these stopping criteria may result in over or undertraining of surrogate models. To overcome these gaps, we propose Global Error-based Learning Function (GELF) for optimal refinement of Kriging surrogate models for the specific purpose of reliability analysis. Instead of prioritizing training points based on their uncertainty and proximity to the limit state like the existing learning functions, GELF for the first time directly and analytically associates the maximum error in the failure probability estimate to the global effect of choosing a candidate training point. This development subsequently facilitates an adaptive training scheme that minimizes the error in adaptive reliability estimation to the highest degree. For this purpose, GELF uses hypothetical future uncertainty information by treating the current construction of the surrogate model as a generative model. The proposed method is tested on three classic benchmark problems and one practical engineering problem. Results indicate that the proposed method has significantly better computational efficiency than the state-of-the-art methods while achieving high accuracy in all the numerical examples.

Key words: *Reliability analysis; Surrogate modeling; Adaptive Kriging; Gaussian process; Global error-based learning function; Error-based stopping criterion*

1. Introduction

Reliability analysis assesses the performance of engineering systems in the presence of uncertainties, which can be aleatory (e.g., natural randomness) or epistemic (e.g., lack of knowledge). The objective of structural reliability analysis is to estimate the probability of a rare event of interest, often the failure of an engineering system, which is determined by a multivariate limit state function that describes the underlying failure mechanisms. The analytic solution of the failure probability P_f is usually in the form of a multifold probability integral, in which the integrand is the joint probability density function (PDF) of the random variables and the domain is determined by the limit state function. The joint PDF may not be available, and the evaluation of the limit state function is often implicit. Therefore, the direct evaluation of this integral is not possible in practical applications. Thus, the failure probability is often "estimated" instead of "calculated".

In the estimation of P_f, the limit state function needs to be evaluated many times given different realizations of the random variables. With advances in science and technology, physical phenomena associated with the limit state functions can be modelled with high fidelity considering various complexities. However, the significant improvement of the model accuracy also gives rise to the more demanding computational cost. Therefore, the estimation of P_f, which requires a significant number of high-fidelity simulations, can be computationally prohibitive in practical engineering problems, especially in the most straight forward type of method, i.e., simulation methods, such as Monte Carlo simulation (MCS) [1]. The estimation of P_f using MCS can be formulated as follows:

$$\hat{P}_f = \frac{n_f}{N_{MCS}} \tag{1}$$

where N_{MCS} is the total number of simulations in the MCS, and n_f is the number of structural failures in the MCS. When P_f is very small, i.e., the failure event is rare, the required N_{MCS} will be very large, hence the prohibitive computational costs. Other simulation methods, such as importance sampling [1] and subset simulation [2], have been proposed to alleviate the computational burden. However, these methods still require a significant number of high-fidelity simulations. Another group of methods for estimating P_f is referred to as approximation methods, such as First

Order Reliability Method (FORM) and Second Order Reliability Method (SORM) [3,4]. These methods can efficiently estimate P_f, however, they often suffer from errors associated with the reduced order approximation of the limit state function, especially when the limit state function is highly nonlinear.

In the last decade, surrogate model methods have become prevalent in the reliability community because of the ability of the surrogate models to achieve balance between accuracy and efficiency. The main idea of methods based on surrogate models is to construct a cheap-to-evaluate model that mimics the behavior of the limit state function. The produced surrogate model will be used subsequently in simulation methods to estimate P_f. To emulate the actual model, a certain number of model evaluations are required, which are also referred to as training points. Kriging [5], among various other surrogate models such as Polynomial Chaos Expansion [6] and Polynomial Response Surface [7–9], has drawn significant more attention because of its built-in capability to provide uncertainty information for its predictions. This uncertainty information is essential, as it can be used in both active learning function and stopping criterion, which are the two most important components in the adaptive reliability analysis methods. The former is used to adaptively select training points to construct the surrogate model, while the latter is used to assess the adequacy of the training process for reliability analysis. Many refer to Kriging-based reliability methods with this adaptive feature as adaptive Kriging methods.

There have been numerous works on adaptive Kriging methods for reliability analysis. Inspired by Efficient Global Optimization [10], Bichon et al. [11] proposed Efficient Global Reliability Analysis (EGRA) with the widely known Efficient Feasibility Function (EFF) that is used as both active learning function and stopping criterion. Echard et al. [5] proposed another popular U learning function in their active learning reliability method that combines Kriging and Monte Carlo Simulation (AK-MCS). Lv et al. [12] proposed the H learning function that is based on information entropy. Yang et al. [13] proposed an Expected Risk Function (ERF) that determines the risk that the sign of a candidate training point is wrongly classified. Sun et al. [14] proposed the Least Improvement Function (LIF) that takes both uncertainty information and joint PDF into account. Wang and Shafieezadeh [15] proposed an Error-based Stopping criterion (ESC) to effectively quantify the error of the Kriging surrogate model when estimating failure probability. In addition, adaptive Kriging methods have also been used in other reliability-related analyses such as reliability-based design optimization [16–19], value of information analysis [20], reliability updating [21,22] and Bayesian updating [23], thanks to Kriging's capability of providing the uncertainty information.

In most existing adaptive Kriging methods, the learning functions are built to consider the proximity of candidate training points to the limit state and the degree of uncertainty. Different learning functions may assign different weights on the two characteristics of the candidate training points. It is reasonable to choose training points that are close to the limit state function and the uncertainty of the assigned sign by the surrogate model is high, as such candidates will have higher probabilities of being wrongly classified to the safe domain or failure domain. However, these learning functions neglect to consider the actual impact of selecting training points. Selecting the candidate with the highest wrong sign estimation probability does not necessarily mean that it will benefit the surrogate model to the highest degree for the purposes of reliability analysis. In addition, existing learning functions evaluate all the candidate training points individually without considering their global impacts. To overcome these challenges and explore how the uncertainty information can be effectively used to assist with the construction of the Kriging surrogate model, we propose a global error-based learning function (GELF) for adaptive Kriging methods. The objective of GELF is to construct a Kriging surrogate model most efficiently and to achieve an acceptable level of error for reliability analysis. Instead of evaluating the learning function for each candidate training point like the existing learning functions, GELF determines the global impact of new training points considering a set of essential candidate training points collectively. The impact is measured using the concept of maximum error of the estimated failure probability, which directly quantifies the quality of the surrogate model.

The rest of this paper is organized into four sections. Section 2 provides a review of adaptive Kriging methods. Section 3 introduces the proposed GELF and the corresponding adaptive Kriging method. The performance of GELF and the proposed method is demonstrated through computational experiments in Section 4. The conclusions are drawn in Section 5.

2. A review of adaptive Kriging methods

This section provides an overview of adaptive Kriging methods for reliability analysis, which is comprised of three subsections on a brief review of Kriging, active learning functions and stopping criteria, respectively.

2. 1 Kriging surrogate model

Let $g(\boldsymbol{x})$ denote the limit state function that is evaluated with a high-fidelity finite element model and $\boldsymbol{x}$ the vector that contains the random variables representing the uncertainty. The Kriging surrogate model for $g(\boldsymbol{x})$ shown by $\hat{g}(\boldsymbol{x})$ can be formulated as follows:

$$\hat{g}(\boldsymbol{x}) = F(\boldsymbol{\beta}, \boldsymbol{x}) + \mathcal{GP}(\boldsymbol{x}) = \boldsymbol{\beta}^T \boldsymbol{f}(\boldsymbol{x}) + \mathcal{GP}(\boldsymbol{x}) \tag{2}$$

where $F(\boldsymbol{\beta}, \boldsymbol{x})$ is the regression component, and $\mathcal{GP}(\boldsymbol{x})$ is a Gaussian process, $F(\boldsymbol{\beta}, \boldsymbol{x})$ is the product of the Kriging basis $\boldsymbol{f}(\boldsymbol{x})$ and corresponding set of coefficients $\boldsymbol{\beta}$. The Gaussian process $\mathcal{GP}(\boldsymbol{x})$ has a zero mean and a covariance matrix. The reader can refer to [24] for the details of construction of the Kriging surrogate model.
The constructed Kriging surrogate model $\hat{g}(\boldsymbol{x})$ follows a normal distribution as follows:

$$\hat{g}(\boldsymbol{x}) \sim N\left(\mu_{\hat{g}}(\boldsymbol{x}), \sigma_{\hat{g}}^2(\boldsymbol{x})\right) \tag{3}$$

where $\mu_{\hat{g}}(\boldsymbol{x})$ is the estimated Kriging mean and $\sigma_{\hat{g}}^2(\boldsymbol{x})$ is the corresponding variance, which represents uncertainty information. In this study, a MATLAB package named UQLab [25] is used to construct the Kriging surrogate model. The codes are extended to implement the proposed learning function.

Kriging's capability of providing uncertainty information can facilitate the adaptive construction process of the surrogate model for reliability analysis. Numerous adaptive Kriging methods have been developed for reliability analysis. Although with many differences, these methods consist of three main components that can affect performance significantly. The first is the active learning function to choose the best training points to construct the surrogate model, the second is the stopping criterion that provides the stop signal for adding new training points, and the third is the simulation method to perform the reliability analysis with the constructed surrogate model. The most commonly used simulation method is Monte Carlo simulation (MCS); however, other simulation methods, such as importance sampling [1] and subset simulation [2], can be used to solve different problems. The use of different simulation methods is not the focus of this study and will not be further discussed. Active learning functions and stopping criteria, however, will be elaborated in the next two subsections.

2.2 Active learning functions

Except for the set of initial training points, all the other training points are selected by the active learning function, thus, active learning functions play an important role in the construction of the surrogate model. Numerous active learning functions have been proposed to efficiently construct the Kriging surrogate model. Two of the most commonly used active learning functions are Expected Learning Function (EFF) [11] and U learning function [5]. The mathematical expression of EFF is as follows:

$$\begin{aligned} EFF(\boldsymbol{x}) &= \int_{a-\epsilon(\boldsymbol{x})}^{a+\epsilon(\boldsymbol{x})} [\epsilon(\boldsymbol{x}) - |a-h|]\phi\big(h; \mu_{GP}(\boldsymbol{x}), \sigma_{GP}(\boldsymbol{x})\big)dh \\ &= \big(\mu_{\hat{g}}(\boldsymbol{x}) - a\big)\left[2\Phi\left(\frac{a-\mu_{GP}(\boldsymbol{x})}{\sigma_{GP}(\boldsymbol{x}^*)}\right) - \Phi\left(\frac{a^- - \mu_{GP}(\boldsymbol{x}^*)}{\sigma_{GP}(\boldsymbol{x}^*)}\right) - \Phi\left(\frac{a^+ - \mu_{GP}(\boldsymbol{x})}{\sigma_{GP}(\boldsymbol{x})}\right)\right] \\ &\quad -\sigma_{\hat{g}}(\boldsymbol{x})\left[2\phi\left(\frac{a-\mu_{GP}(\boldsymbol{x})}{\sigma_{GP}(\boldsymbol{x})}\right) - \phi\left(\frac{a^- - \mu_{GP}(\boldsymbol{x}^*)}{\sigma_{GP}(\boldsymbol{x}^*)}\right) - \phi\left(\frac{a^+ - \mu_{GP}(\boldsymbol{x})}{\sigma_{GP}(\boldsymbol{x})}\right)\right] \\ &\quad +2\sigma_{GP}(\boldsymbol{x})\left[\Phi\left(\frac{a^+ - \mu_{GP}(\boldsymbol{x})}{\sigma_{GP}(\boldsymbol{x})}\right) - \Phi\left(\frac{a^- - \mu_{GP}(\boldsymbol{x})}{\sigma_{GP}(\boldsymbol{x})}\right)\right] \end{aligned} \tag{4}$$

where $\phi(\cdot)$ is the standard Gaussian probability density function (PDF), Φ is the standard Gaussian cumulative density function (CDF), $a = 0$, $\epsilon(\boldsymbol{x}) = 2\sigma_{\hat{g}}(\boldsymbol{x})$, $a^+ = a + \epsilon(\boldsymbol{x})$ and $a^- = a - \epsilon(\boldsymbol{x})$. The term $[\epsilon(\boldsymbol{x}) - |a-h|]$ measures the proximity of the untried point to the limit state $g(\boldsymbol{x}) = a$, and is weighted by the term $\phi(h; \mu_{\hat{g}}(\boldsymbol{x}), \sigma_{\hat{g}}(\boldsymbol{x}))$. U learning function has the following mathematical expression:

$$U(\boldsymbol{x}^*) = \frac{\left|\mu_{\hat{g}}(\boldsymbol{x})\right|}{\sigma_{\hat{g}}(\boldsymbol{x})} \tag{5}$$

There are many other active learning functions, e.g., H learning function [12], Expected Risk Function (ERF) [13] and Least Improvement Function (LIF) [14] to name a few. Most existing active learning functions aim to find training points that are close to the predicted limit state and have higher uncertainty, as these points are more prone to be wrongly classified as failed or safe. Different active learning functions may assign different weights to the proximity and uncertainty. For instance, the U learning function tends to assign a higher weight to points close to the predicted limit state rather than those that are further away but have higher uncertainty compared to EFF. Choosing the points that have higher probabilities of being wrongly classified can help to correct the potential error of the surrogate model, however, it not necessarily the most effective manner to improve the overall accuracy of the surrogate model. In addition, when choosing a training point, all the candidate points are evaluated using the active learning function individually, that is, the impact of adding the selected training point to the entire surrogate model is not fully considered. In this study, a novel active learning function is proposed that considers the global impact of candidate training points. This learning function will be introduced in Section 3.

2.3 Stopping criteria

Another key component in adaptive Kriging methods is the stopping criterion. A loose stopping criterion can lead to an inaccurate surrogate model that cannot provide an accurate estimate of failure probability. On the other hand, an overly conservative one may lead to unnecessary training. A commonly used approach is to check the value of the chosen active learning function for all the candidate points against a predefined threshold. For instance, if the U learning function is used for training, no new training points are needed when the U learning function values for all the candidate training points are larger than 2. This type of stopping criterion works, as it often guarantees that all the candidate training points have a low probability of wrong classification. However, not all stopping criteria that depend on values of active learning functions have physical or statistical meaning, and the threshold value can be subjective. In Wang and Shafieezadeh [15], it was shown that stopping criterion based on both U learning function and EFF can lead to significant over or undertraining. To address this challenge, an efficient error-based stopping criterion (ESC) was proposed in Wang and Shafieezadeh [15]. In ESC, the maximum error rate $\hat{\epsilon}_{max}$ of the estimated probability of failure was derived and used as the stopping criterion for the construction of the surrogate model. This maximum error rate can be estimated using the following equation:

$$\hat{\epsilon}_{max} = max\left(\left|\frac{\widehat{N}_f}{\widehat{N}_f - \hat{S}_f^u} - 1\right|, \left|\frac{\widehat{N}_f}{\widehat{N}_f + \hat{S}_s^u} - 1\right|\right) \tag{6}$$

where $\widehat{N}_f$ is the estimated number of points in the failure domain out of the entire candidate training point population by the surrogate model, $\hat{S}_f$ is the total number of wrong sign estimations in the estimated failure domain $\widehat{\Omega}_f$ by the surrogate model, and $\hat{S}_s$ is the one in estimated safe domain $\widehat{\Omega}_s$ by the surrogate model, $\hat{S}_f^u$ and $\hat{S}_s^u$ are the upper bounds of $\hat{S}_f$ and $\hat{S}_s$, respectively. In Wang and Shafieezadeh [15], it was found that both $\hat{S}_s$ and $\hat{S}_f$ follow Poisson binomial distributions with means and variances shown below:

$$\hat{S}_s \sim PB\left(\sum_{i=1}^{\widehat{N}_s} P_i^{wse}, \sum_{i=1}^{\widehat{N}_s} P_i^{wse}\left(1 - P_i^{wse}\right)\right) \tag{7}$$
$$x_i \in \widehat{\Omega}_s$$

$$\hat{S}_f \sim PB\left(\sum_{i=1}^{\widehat{N}_f} P_i^{wse}, \sum_{i=1}^{\widehat{N}_f} P_i^{wse}\left(1 - P_i^{wse}\right)\right) \tag{8}$$
$$x_i \in \widehat{\Omega}_f$$

where PB represents the Poison Binomial distribution and P_i^{wse} is the probability of wrong sign estimation for x_i,

which can be computed as $P_i^{wse} = \Phi\left(-\frac{|\mu_{\hat{g}}(\boldsymbol{x})|}{\sigma_{\hat{g}}(x)}\right)$, where $\Phi(\cdot)$ is the standard Gaussian cumulative density function. Thus, the upper and lower bounds of $\hat{S}_s$ and $\hat{S}_f$ with a confidence level α can be found as:

$$\hat{S}_s \in \left(\boldsymbol{\theta}_{\hat{S}_s}^{-1}\left(\frac{\alpha}{2}\right), \boldsymbol{\theta}_{\hat{S}_s}^{-1}\left(1-\frac{\alpha}{2}\right)\right) \tag{9}$$

$$\hat{S}_f \in \left(\boldsymbol{\theta}_{\hat{S}_f}^{-1}\left(\frac{\alpha}{2}\right), \boldsymbol{\theta}_{\hat{S}_f}^{-1}\left(1-\frac{\alpha}{2}\right)\right) \tag{10}$$

where $\boldsymbol{\theta}_{\hat{S}_s}^{-1}$ and $\boldsymbol{\theta}_{\hat{S}_f}^{-1}$ are the inverse CDF of the Poisson binomial distributions in Eq. (7) and (8). The reader is referred to Wang and Shafieezadeh [15] for more details. The estimate of the maximum error $\hat{\epsilon}_{max}$ provides very useful information on how accurate the constructed Kriging surrogate model is in terms of estimating the failure probability. A threshold ϵ_{thr} can be set as 5%. When $\hat{\epsilon}_{max} \leq \epsilon_{thr}$, it indicates the Kriging surrogate model is accurate enough and no more training points are needed. ESC has been proven very effective in many studies [19,20,26,27]. Albeit with its efficacy, ESC only contributes to the stopping criterion component. In this study, the concept behind ESC is extended to facilitate the selection of the training point as well. The proposed active learning function and method are introduced in the next section.

3. Adaptive Kriging Reliability Method with an Error-Based Learning Function

In this study, we propose a novel adaptive Kriging reliability method with a global error-based learning function (AK-GELF-MCS) that aims to overcome the challenges mentioned in Section 2.2.

3.1 Global Error-Based Learning Function

The main objective of our proposed GELF is to identify the training point that can have the greatest global impact on the surrogate model given it is added to the surrogate model. The first important question is: how do we know if the impact of adding a new training point is even good? The most existing learning functions to choose the training point evaluate the candidate training points individually and are not able to capture the global impact. To achieve the greatest efficiency and accuracy, a more explicit and objective goal of the learning function is needed. Here in this study, we propose to utilize ESC, a stopping criterion that has been proven effective, as the signal of the quality of the surrogate model, that is, we want to choose the training points that reduce the maximum error in ESC. ESC is measured using the pool of the candidate training points and the change of ESC can reflect the global impact. Here comes the second important question: how do we measure the ESC of adding a training point before evaluating it? This is possible with the hypothetical future variance.

Assume we have a Kriging surrogate constructed with m training points denoted as $\hat{g}_P(\boldsymbol{x}) = \hat{g}\left(\boldsymbol{x}|\{\boldsymbol{x}^{(i)}\}_{i=1}^{m}\right)$. It follows the Gaussian distribution as follows:

$$\hat{g}_P(\boldsymbol{x}) \sim N(\mu_P(\boldsymbol{x}), \sigma_P^2(\boldsymbol{x})) \tag{11}$$

where $\boldsymbol{x}$ can be any point, $\mu_P(0,\boldsymbol{x})$ is the mean and $\sigma_P^2(0,\boldsymbol{x})$ is the variance for the current construction of the surrogate model. Let us assume that a hypothetical future Kriging surrogate is constructed with the current m training points and a potential future training point $\boldsymbol{x}^{m+1}$. Let y^F denote the hypothetical future simulated prediction at $\boldsymbol{x}^{m+1}$. It is obvious that y^F follows $N(\mu_P(\boldsymbol{x}^{m+1}), \sigma_P^2(\boldsymbol{x}^{m+1}))$. Therefore, a hypothetical future surrogate model at any $\boldsymbol{x}$ follows the Gaussian distribution as follows:

$$\hat{g}_F\left(\boldsymbol{x}|\{\boldsymbol{x}^{(i)}\}_{i=1}^{m+1}, y^F\right) \sim N(\mu_F\left(\boldsymbol{x}|\{\boldsymbol{x}^{(i)}\}_{i=1}^{m+1}, y^F\right), \sigma_F^2(\boldsymbol{x}|\{\boldsymbol{x}^{(i)}\}_{i=1}^{m+1}, y^F)) \tag{12}$$

where the hypothetical future mean $\mu_F\left(\boldsymbol{x}|\{\boldsymbol{x}^{(i)}\}_{i=1}^{m+1}, y^F\right)$ follows a Gaussian distribution whose mean is still $\mu_P(\boldsymbol{x})$, and the hypothetical future variance $\sigma_F^2(\boldsymbol{x}|\{\boldsymbol{x}^{(i)}\}_{i=1}^{m+1}, y^F)$ depends only on $\boldsymbol{x}^{m+1}$ and thus is replaced with $\sigma_F^2(\boldsymbol{x}|\{\boldsymbol{x}^{(i)}\}_{i=1}^{m+1})$. It is worth noting that we do not need any new evaluations of the finite element model or optimization of the parameter $\boldsymbol{\theta}$. However, we do need to recalculate the correlation $\boldsymbol{r}(\boldsymbol{x})$ and autocorrection matrix

$\boldsymbol{R}(\boldsymbol{x})$, of which the computational costs are negligible compared with the expensive-to-evaluate limit state function. Therefore, in each iteration, we can construct the hypothetical future surrogate model for any candidate training point. Note that this definition has been applied in conjunction with existing learning functions such as EFF in two multi-fidelity reliability analysis methods [28,29]. However, in this study, the definition is utilized in a more meaningful way where the global impact regarding the maximum error is quantified by the proposed learning function, which will be introduced as follows.

As the hypothetical future prediction y^F follows $N(\mu_P(\boldsymbol{x}^{m+1}), \sigma_P^2(\boldsymbol{x}^{m+1}))$, assuming that the hypothetical future mean $\mu_F\left(\boldsymbol{x}|\{\boldsymbol{x}^{(i)}\}_{i=1}^{m+1}, y^F\right)$ stays the same as that of the present model $\mu_P(\boldsymbol{x})$, the hypothetical wrong sign estimation for any candidate training point $\boldsymbol{x}$ given a selected training point $\boldsymbol{x}^{m+1}$ can be calculated as follows:

$$P_{i,F}^{wse}(\boldsymbol{x}|\boldsymbol{x}^{m+1}) = \Phi\left(-\frac{|\mu_P(\boldsymbol{x})|}{\sigma_F\left(\boldsymbol{x}|\{\boldsymbol{x}^{(j)}\}_{j=1}^{m+1}\right)}\right)$$

Accordingly, the hypothetical future total number of wrong sign estimations in the estimated failure domain $\hat{\Omega}_f$, $\hat{S}_f$, and the one in estimated safe domain $\hat{\Omega}_s$, $\hat{S}_{f,F}$, follow the following distributions:

$$\hat{S}_{s,F}(\boldsymbol{x}^{m+1}) \sim PB\left(\sum_{i=1}^{\widehat{N}_s} P_{i,F}^{wse}(\boldsymbol{x}|\boldsymbol{x}^{m+1}) \ , \sum_{i=1}^{\widehat{N}_s} P_{i,F}^{wse}(\boldsymbol{x}|\boldsymbol{x}^{m+1})\left(1 - P_{i,F}^{wse}(\boldsymbol{x}|\boldsymbol{x}^{m+1})\right)\right) \tag{13}$$
$$\boldsymbol{x}_i \in \hat{\Omega}_s$$

$$\hat{S}_{f,F}(\boldsymbol{x}^{m+1}) \sim PB\left(\sum_{i=1}^{\widehat{N}_f} P_{i,F}^{wse}\ (\boldsymbol{x}|\boldsymbol{x}^{m+1}) \ , \sum_{i=1}^{\widehat{N}_f} P_{i,F}^{wse}\left(1 - P_{i,F}^{wse}(\boldsymbol{x}|\boldsymbol{x}^{m+1})\ \right)\right) \tag{14}$$
$$\boldsymbol{x}_i \in \hat{\Omega}_f$$

Note that as the assumption that the hypothetical future mean $\mu_F\left(\boldsymbol{x}|\{\boldsymbol{x}^{(i)}\}_{i=1}^{m+1}, y^F\right)$ stays the same as that of the present model $\mu_P(\boldsymbol{x})$, the hypothetical future estimated failure and safe domains stay the same as $\hat{\Omega}_f$ and $\hat{\Omega}_s$, respectively. Accordingly, the hypothetical future estimated total numbers of points in the failure and safe domains are still $\widehat{N}_f$ and $\widehat{N}_s$, respectively. Therefore, the upper and lower bounds of $\hat{S}_{s,F}$ and $\hat{S}_{f,F}$ with a confidence level α can be found as:

$$\hat{S}_{s,F}(\boldsymbol{x}^{m+1}) \in \left(\boldsymbol{\Theta}^{-1}_{\hat{S}_{s,F}(\boldsymbol{x}^{m+1})}\left(\frac{\alpha}{2}\right), \boldsymbol{\Theta}^{-1}_{\hat{S}_{s,F}(\boldsymbol{x}^{m+1})}\left(1-\frac{\alpha}{2}\right)\right) \tag{15}$$

$$\hat{S}_{f,F}(\boldsymbol{x}^{m+1}) \in \left(\boldsymbol{\Theta}^{-1}_{\hat{S}_{f,F}(\boldsymbol{x}^{m+1})}\left(\frac{\alpha}{2}\right), \boldsymbol{\Theta}^{-1}_{\hat{S}_{f,F}(\boldsymbol{x}^{m+1})}\left(1-\frac{\alpha}{2}\right)\right) \tag{16}$$

where $\boldsymbol{\Theta}^{-1}_{\hat{S}_{s,F}(\boldsymbol{x}^{m+1})}$ and $\boldsymbol{\Theta}^{-1}_{\hat{S}_{f,F}(\boldsymbol{x}^{m+1})}$ are the inverse CDF of the Poisson binomial distributions in Eq. (13) and (14). For any new candidate training point $\boldsymbol{x}^{m+1}$, the corresponding hypothetical future ESC can be evaluated and used as the active learning function to select the next best training point. The candidate training point with the smallest hypothetical future ESC can be selected. Thus, a GELF can be formulated as follows:

$$GELF(\boldsymbol{x}^{m+1}) = max\left(\left|\frac{\widehat{N}_f}{\widehat{N}_f - \hat{S}^u_{f,F}(\boldsymbol{x}^{m+1})} - 1\right|, \left|\frac{\widehat{N}_f}{\widehat{N}_f + \hat{S}^u_{s,F}(\boldsymbol{x}^{m+1})} - 1\right|\right) \tag{17}$$

The proposed GELF is the first learning function that associates the effect of candidate training points directly to the maximum error of the failure probability estimation. Instead of trying to find the training points that have larger uncertainties and are close to the limit state like the existing learning functions, GELF aims to find the training points that directly lower the maximum error caused by the surrogate model to the highest degree. GELF utilizes the concept

of hypothetical future variance and collectively evaluates the candidate training points instead of evaluating each candidate training point individually, thus enabling the consideration of the global impact. In the next subsection, the adaptive Kriging method with the proposed GELF is introduced.

3.2 Application process of the proposed method

The proposed GELF can be easily incorporated in the adaptive Kriging framework. The flowchart of the approach is shown in Fig. 2. In Step 1, set of candidate training points, denoted as $\boldsymbol{S}$, of the size of N_{MCS} is generated using Latin Hypercube sampling. In Step 2, Randomly select N_i initial training points (N_i is determined as $\min\{12, (D+1)(D+2)/2\}$) from $\boldsymbol{S}$. Evaluate the N_i points using computational, e.g., finite element, models to get the initial training point set $\{\boldsymbol{x}^{(i)}\}_{i=1}^{m=N_i}$. Afterwards in Step 3, construct the Kriging surrogate model $\hat{g}\left(\boldsymbol{x}|\{\boldsymbol{x}^{(i)}\}_{i=1}^{N_i}\right)$ with the current set of training points $\{\boldsymbol{x}^{(i)},\}_{i=1}^{m}$. Then, the responses $\mu_P(\boldsymbol{x})$ are obtained from the Kriging surrogate model $\hat{g}\left(\boldsymbol{x}|\{\boldsymbol{x}^{(i)},\}_{i=1}^{N_i}\right)$ for every candidate training point in $\boldsymbol{S}$. According to responses $\mu_P(\boldsymbol{x})$, the failure probability $\hat{P}_f$ can be estimated via MCS. However, it is not guaranteed that the surrogate model is sufficiently accurate for the reliability analysis. Thus, the ESC as follows needs to be checked:

$$\hat{\epsilon}_{max} < 5\% \tag{18}$$

If the ESC is satisfied, move to Step 6 to check the sufficiency of the population of $\boldsymbol{S}$ using the criterion as follows:

$$COV_{\hat{P}_f} = \sqrt{\frac{1-\hat{P}_f}{N_{MCS}\hat{P}_f}} \tag{19}$$

If $COV_{\hat{P}_f}$ is smaller than 5%, go to Step 9 and report the failure probability. Otherwise, an additional number N_{Δ_S} of candidate training points should be added to $\boldsymbol{S}$, and the process should move back to Step 4. If in Step 5 the ESC is not satisfied, new training point needs to be added using $GELF$ in Step 7. Afterwards in Step 8, update the set of training points with the best training point identified in Step 7, and then go back to Step 3.

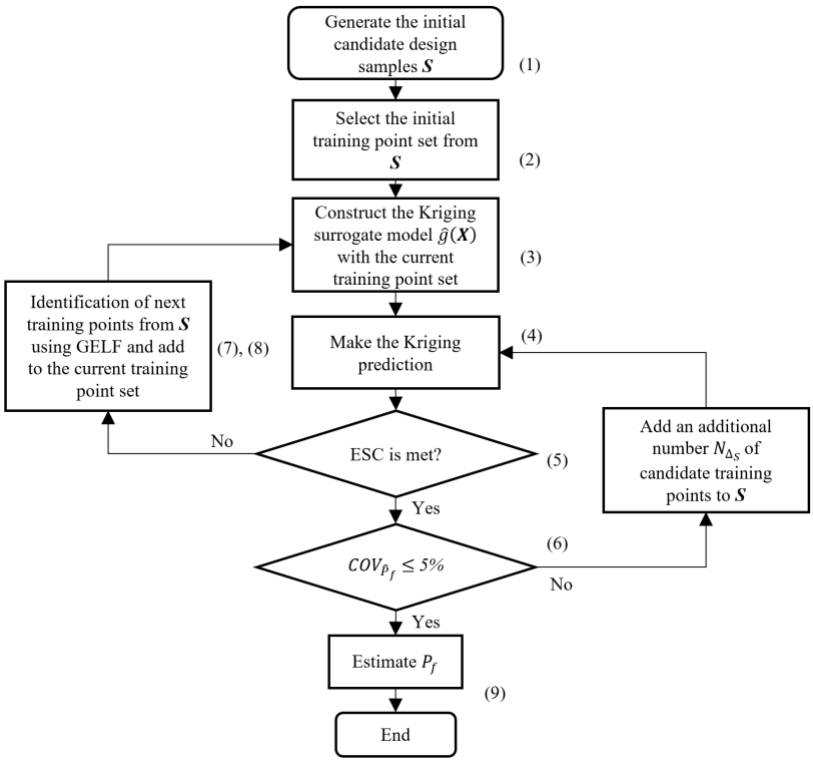

Fig. 2 Flowchart of the proposed method

The proposed method uses GELF to select the training point that aims to lower the estimated maximum error of the surrogate model most efficiently while considering the global impact of adding the training point. Note that it is not advised to construct the hypothetical future surrogate model for every candidate training point, although the cost of constructing a hypothetical future surrogate model is negligible, each evaluation of GELF will require the hypothetical future surrogate model to be evaluated N_{mcs} times. If every candidate training point is evaluated using GELF, a total number of N_{mcs}^2 evaluations of Kriging surrogate model is needed, of which the computational costs can increase significantly when the required N_{mcs} increases for problems with small failure probability. Therefore, we propose to use a set of essential candidate training points. The essential candidate training points can be selected based on any learning function. EFF is used in this study for the selection of essential candidate training points. It is found that the larger the essential candidate training point set, the better the performance of the proposed method. However, a larger set will also increase the computational cost. Based on our numerical investigations, we found that 2,000 essential candidate training points are sufficient. In addition, the impact of the value of N_e is investigated through the computational experiments in Section 4.

4. Computational experiments

To evaluate the performance of $GELF$ and the proposed method, four computational experiments, including three classic benchmark problems and one practical engineering problem, are investigated. These computational experiments have at least one of the following properties: highly nonlinear, non-differentiable, and high-dimensional. The performance of the proposed method is compared with AK-MCS [5] with ESC [15], which is referred to as AK-MCS-ESC, and Polynomial Chaos Kriging using EFF as the learning function and the beta stability (0.005) as the stopping criterion as in [30], which is referred to as PCK-EFF-BS. All the computational experiments are repeated 20 times.

4.1 Example 1: 2D problem

The first example is based on a classical two dimensional problem investigated in many studies [31,32]. The limit state function is shown as follows:

$$g(x_1, x_2) = -1 + (0.9063x_1 + 0.4226x_2 - 6)^2 + (0.9063x_1 + 0.4226x_2 - 6)^3 \\ -0.6(0.9063x_1 + 0.4226x_2 - 6)^4 + (0.4226x_1 - 0.9063x_2) \quad (20)$$

where x_1 follows a uniform distribution between 4.5 and 7.5, and x_2 follows a uniform distribution between 4.7 and 7.7. The proposed method AK-GELF-ESC is applied, and the results are compared with the other state-of-the-art methods. The results of the reliability analyses are summarized in Table 1. Note that the beta stability threshold for PCK-EFF-BS is changed to $5 \cdot 10^{-4}$ after observing the accuracy of the method for this problem, as the threshold of 0.005 which is stated in [30] to be an appropriate value will yield extremely large errors. The boxplots for the training point numbers and errors are presented in Fig. 3. It can be observed that the proposed method requires around 28% fewer training points to converge compared to AK-MCS-ESC. Also, the average error of the proposed method is lower than the other methods. Both the efficiency and accuracy of analysis are improved by taking advantage of the proposed error-based learning function. PCK-EFF-BS costs the most training points, albeit with a more conservative threshold, but cannot guarantee the robustness of convergence.

Fig. 4 shows the error trend comparison of AK-GELF-ESC and AK-MCS-ESC with the same set of initial training points. The proposed method converges significantly faster than AK-MCS-ESC. The distribution of the initial training points and the added training points are shown in Fig. 5. It is noted that both AK-GELF-ESC and AK-MCS-ESC can construct an accurate surrogate model, while the proposed method requires fewer training points.

Table 1 Reliability results for Example 1

Method	Average number of training points (Standard deviation)	P_f (Standard deviation)	Average error* (Standard deviation)
MCS	-	7.09×10^{-3}	-
AK-GELF-ESC	36.75 (5.24)	7.16×10^{-3} (2.43×10^{-4})	0.60% (0.54%)
AK-MCS-ESC	50.05 (8.00)	7.03×10^{-3} (2.71×10^{-4})	1.01% (1.14%)
PCK-EFF-BS	55.35(15.92)	7.23×10^{-3} (6.99×10^{-4})	4.29% (8.06%)

*: denoting the average of the errors incurred by the surrogate model (compared with crude MCS) for 20 runs.

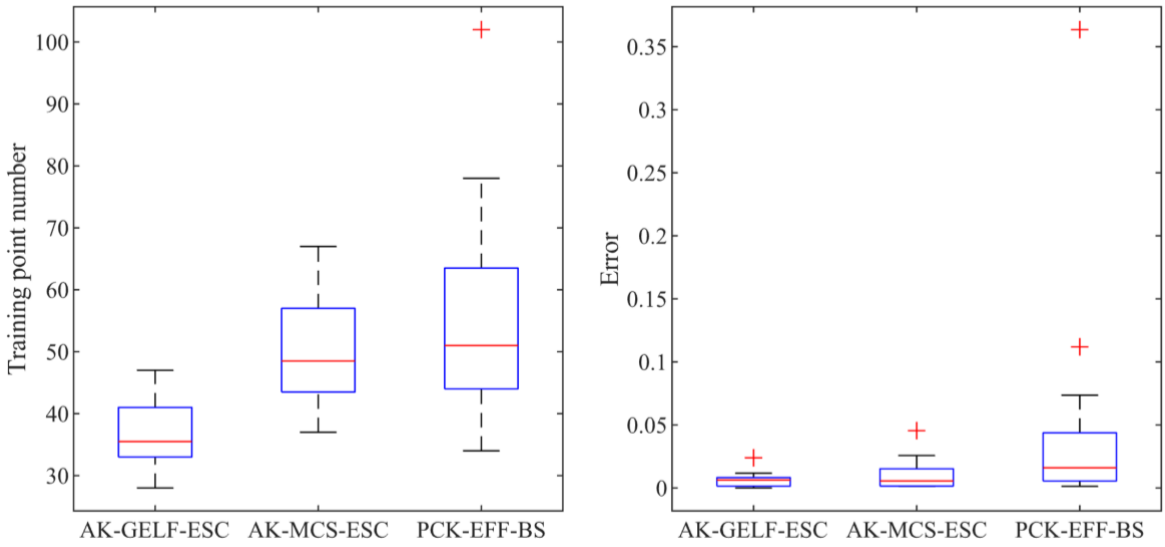

Fig. 3 The comparison of different methods for Example 1

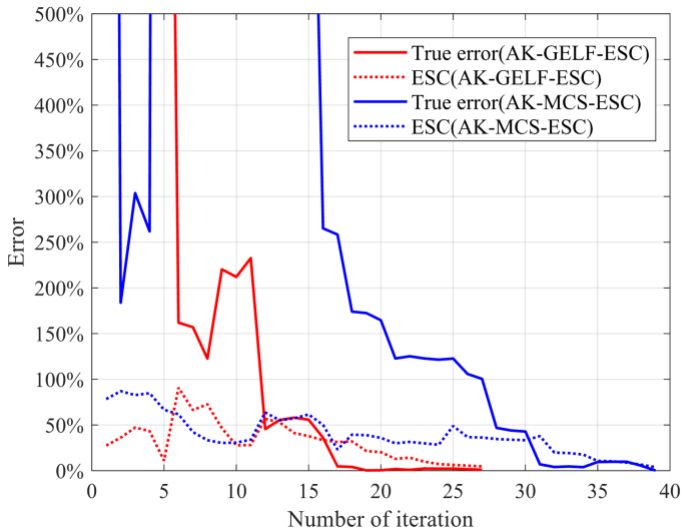

Fig. 4 The comparison of error trends for Example 1

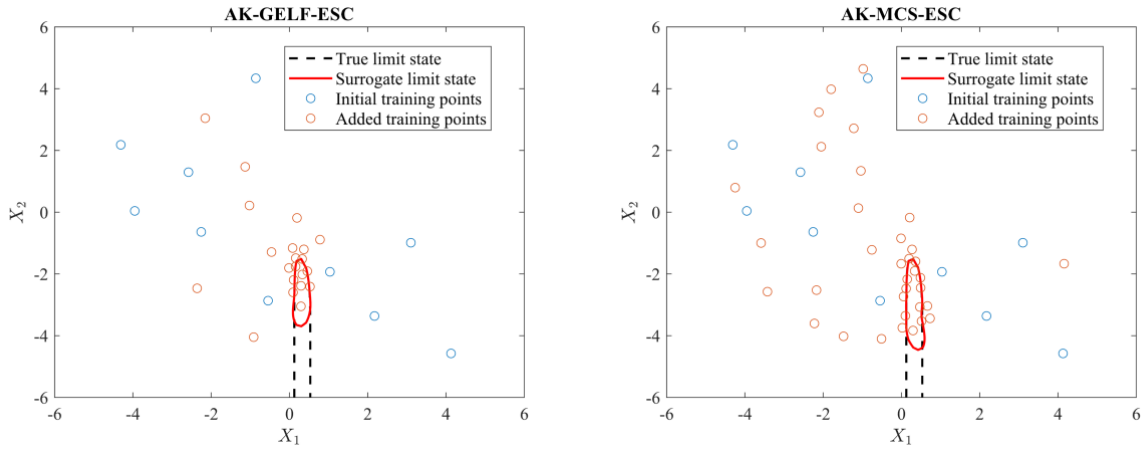

Fig. 5 The comparison of contours in the standard normal space for Example 1

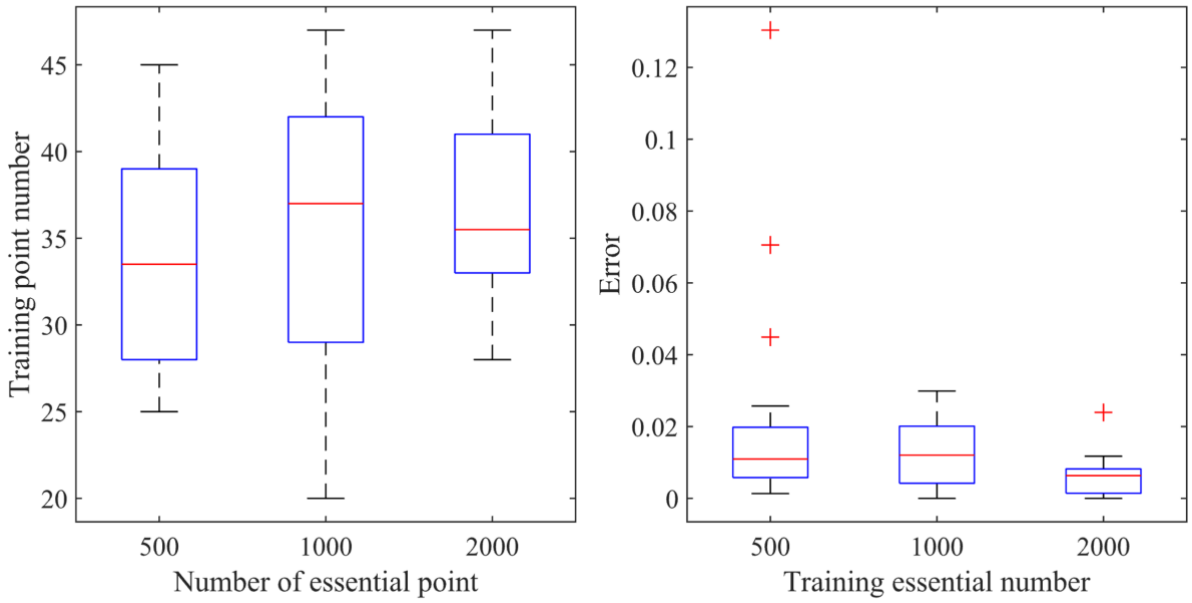

Fig. 6 The results for the proposed method with different numbers of essential points

A parametric study on the number of essential points is performed for this example. The results are presented in the boxplots in Fig. 6. It can be observed that with a larger number of essential candidate training points, the proposed method will provide more stable results.

4.2 Example 2: Oscillator problem

The second example is an undamped single degree of freedom system as shown in Fig. 7. This problem has been investigated in many studies [2,5,33–35]. The limit state function is described below:

$$g(c_1, c_2, m, r, t_1, F_1) = 3r - \left| \frac{2F_1}{m\omega_0^2} sin\left(\frac{\omega_0 t_1}{2}\right) \right| \tag{21}$$

where $\omega_0 = \sqrt{\frac{c_1+c_2}{m}}$ is the system frequency. There are six random variables in the limit state function. The probabilistic descriptions of the six random variables are presented in Table 2.

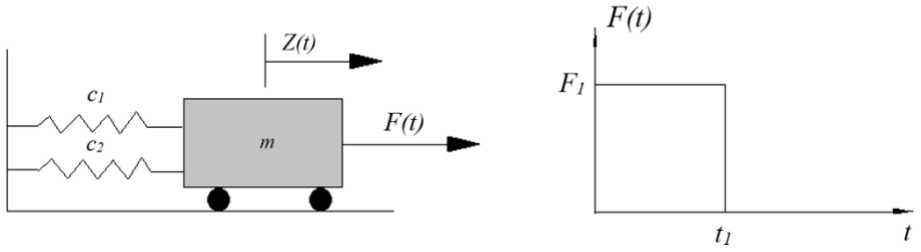

Fig. 7 Oscillator

The proposed method is applied and compared with the other state-of-the-art methods. Table 3 summarizes the results of reliability analysis by different methods, and Fig. 8 presents the boxplots for the number of training points and errors. For this example, AK-GELF-ESC performs better than AK-MCS-ESC in both accuracy and efficiency. The proposed method uses around 90% of the training points of AK-MCS-ESC to achieve an average error that is 46% smaller. PCK-EFF-BS, albeit with a similar number of training points compared to AK-GELF-ESC, has a much larger error than the other methods.

Table 2 Random variables in the oscillator

Random variable	Distribution	Mean	Standard deviation
m	Normal	1	0.05
k_1	Normal	1	0.1
k_2	Normal	0.1	0.01
r	Normal	0.65	0.05
F_1	Normal	1	0.2
t_1	Normal	1	0.2

Table 3 Reliability results for Example 2

Method	Average number of training points (Standard deviation)	$\boldsymbol{P_f}$ (Standard deviation)	Average error* (Standard deviation)
MCS	-	2.85×10^{-2}	-
AK-GELF-ESC	30.55(3.51)	2.87×10^{-3} (0.92×10^{-4})	1.33% (1.25%)
AK-MCS-ESC	34.15(3.85)	2.88×10^{-3} (1.38×10^{-3})	2.88% (1.93%)
PCK-EFF-BS	29.55(10.49)	2.91×10^{-3} (3.42×10^{-3})	6.5% (10.25%)

*: denoting the average of the errors incurred by the surrogate model (compared with crude MCS) for 20 runs.

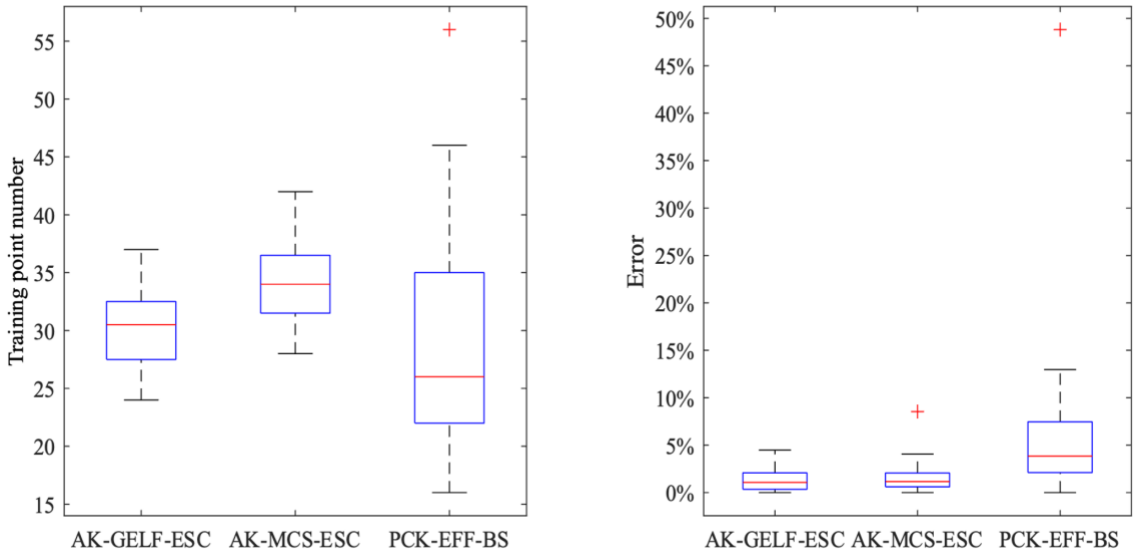

Fig. 8 The comparison of different methods for Example 2

4.2 Example 3: 10-Dimensional problem

The third problem is a 10-dimensional problem that has been studied in [5,36,37]. The limit state function is shown as follows:

$$g(x_1, \dots, x_n) = \left(n + 3\sigma\sqrt{n}\right) - \sum_{i=1}^{n} x_i \tag{22}$$

where all the random variables x_is, follow independent lognormal distributions with a mean of 1 and a standard deviation of 0.2, and n is set to be 10. The proposed method is applied and compared with the other state-of-the-art methods. The results of reliability analysis by different methods are summarized in Table 4. The boxplots for the number of training points and errors are presented in Fig. 9. For this example, AK-GELF-ESC and AK-MCS-ESC have very similar computational costs; however, the average error of the proposed method is only around 40% of that of AK-MCS-ESC. On the other hand, PCK-EFF-BS uses only 52.4 training points on average, but the errors are extremely high, which indicates that the beta stability may not be a good stopping criterion for all the problems.

Table 4 Reliability results for Example 3

Method	Average number of training points (Standard deviation)	$\boldsymbol{P_f}$ (Standard deviation)	Average error* (Standard deviation)
MCS	-	2.7×10^{-3}	-
AK-GELF-ESC	67.85(8.31)	2.75×10^{-3} (1.14×10^{-4})	1.4% (1.03%)
AK-MCS-ESC	68.1(9.96)	2.84×10^{-3} (9.34×10^{-5})	3.42% (2.01%)
PCK-EFF-BS	52.4(22.01)	2.43×10^{-3} (8.83×10^{-4})	20.68% (26.74%)

*: denoting the average of the errors incurred by the surrogate model (compared with crude MCS) for 20 runs.

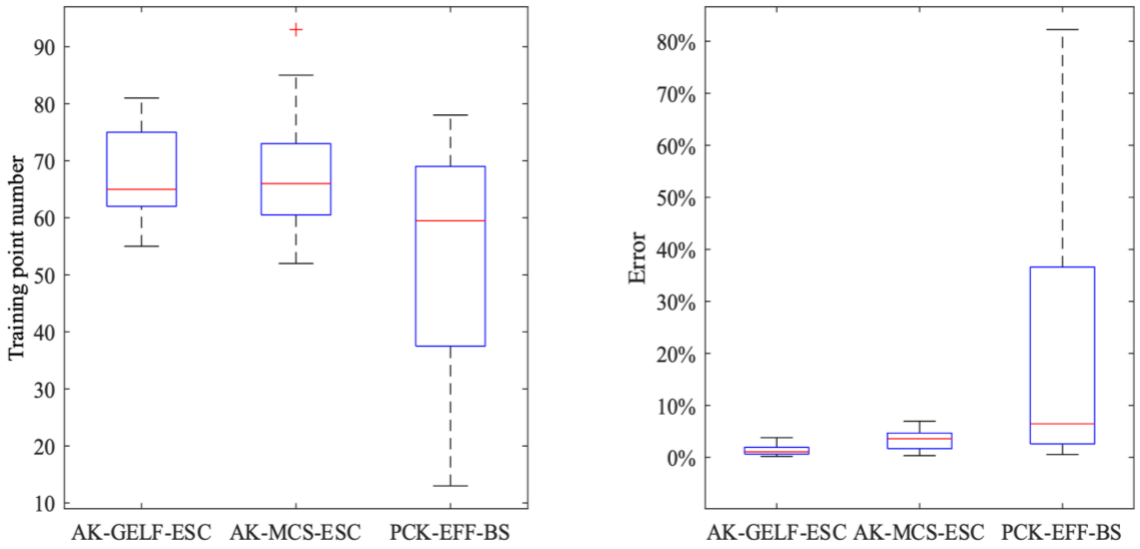

Fig. 9 The comparison of different methods for Example 3

4.4 Example 4: Natural gas pipeline problem

The last numerical example is a practical engineering problem related to a natural gas pipeline. Natural gas pipelines and networks are essential infrastructure that transport and distribute natural gas over long distances. The failure of pipelines may lead to significant impacts on the economy, environment and society [38]. Therefore, the reliability of pipelines is a major concern. The existing data indicate that corrosion is one of the main causes for the failure of gas pipelines [39,40]. For instance, 38.5% and 26.5% recorded failures of gas transmission pipelines are caused by corrosion according to the Lithuanian and European Gas pipeline Incident data Group (EGIG) databases, respectively [39,40]. The operational data also reveal that local pitting corrosion, which is typically a high density of corrosion pits in a small area, is responsible for a large percentage of through-wall defects. Reduction of the pipe wall thickness under local pitting corrosion may lead to high stress concentrations in the pipe wall and eventually cause the rupture of the pipe. The objective of this numerical example is to investigate the reliability of a natural gas pipeline with such local pits or defects. A finite element model is constructed to model the natural gas pipe with a defected zone using similar settings as the one in [38]. The key parameters of the pipe model can be found in Table 5.

Table 5 Detailed parameters of the pipe

Description	Distribution	Mean	COV
Pressure	Uniform	4.5 MPa	21.28%
Pipe thickness	Lognormal	14.3	5%
Elastic modulus	Lognormal	$2.0 \cdot 10^5$ MPa	5%
Crack depth	Uniform	5.5 mm	37.14%
Pipe diameter	Deterministic	1220 mm	-
Crack length	Deterministic	200 mm	-
Crack width	Deterministic	6.7 mm	-
Ultimate von Mises stress	Deterministic	612 MPa	-

Referring to existing work [41,42] this engineering application adopts the von Mises (distortion energy) theory in ANSYS software to analyze the stress distribution of the defected pipe. When the von Mises stress reaches the ultimate stress throughout the defected area, the corresponding applied internal pressure can be defined as the failure pressure and failure event is considered to occur. Keeping consistency with the existing works [38,43], this example adopts SHELL element to model the pipe structure, and the reduced thickness SHELL element is used to model the defect. To balance the accuracy and efficiency, the defected and the adjacent areas are meshed with a smaller element size. The pressure load is applied uniformly to the inside face of the pipe. Fig. 10 illustrates the finite element model of the pipe. As the primary focus of this application lies in validating the performance of the proposed method, some

reasonable simplifications are made in the modeling process, such as the corrosion degree is directly reflected in the random variable of crack depth, instead of modeling the chemical and physical process.

The proposed method with 2,000 essential candidate training points is performed and compared with the other state-of-the-art methods. The results of reliability analysis by different methods are summarized in Table 6. For this problem, the reference result by MCS is not available due to the extremely high computational costs. Thus, the errors are not reported here. We can still observe that while the proposed method and AK-MCS-ESC reach very close estimates of failure probability, the proposed method requires nearly 20% fewer training points compared to AK-MCS-ESC and achieves more stable results. From the boxplots in Fig. 11, it can also be shown that PCK-EFF-BS produces unstable results, as the beta stability stops training too early.

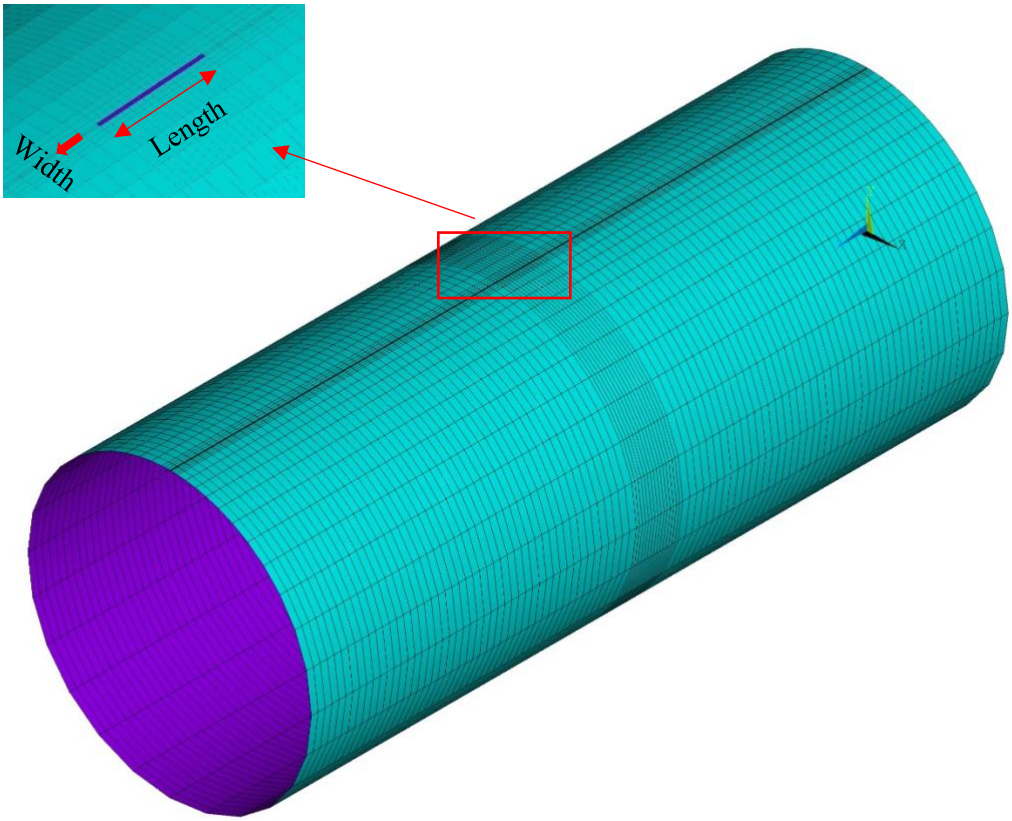

Fig. 10 Illustration of the finite element model for the defected pipe

Table 6 Reliability results for Example 4

Method	Average number of training points (Standard deviation)	P_f (Standard deviation)
AK-GELF-ESC	37.0 (5.2)	1.86×10^{-3} (8.45×10^{-5})
AK-MCS-ESC	45.5 (6.3)	1.87×10^{-3} (7.48×10^{-5})
PCK-EFF-BS	28.9 (6.8)	1.65×10^{-3} (5.30×10^{-4})

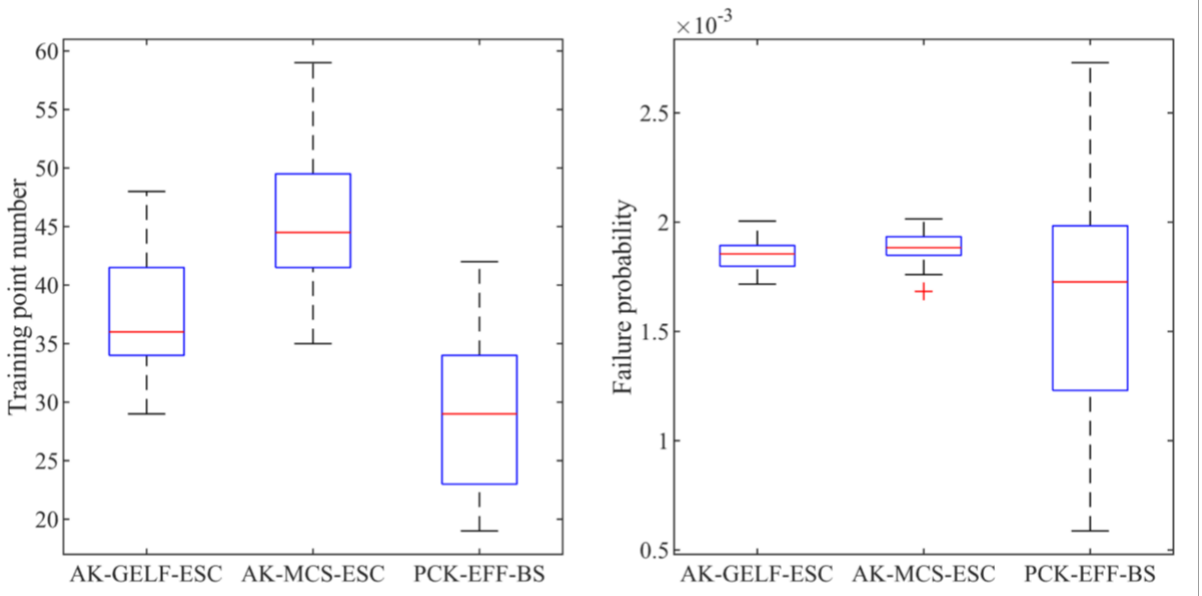

Fig. 11 The comparison of different methods for Example 4

6. Conclusions

How to efficiently construct an accurate Kriging surrogate model for reliability analysis has been a major problem in Kriging-assisted reliability analysis. Various active learning functions have been developed, which try to find the training points that help construct the Kriging surrogate model. In this study, we propose a global error-based learning function that takes an alternative approach than the one in the other studies. Instead of trying to locate the training points that have large uncertainties and are close to the limit state, the proposed method aims to find the training points that directly lower the maximum error of the Kriging-based reliability estimate by considering the future hypothetical uncertainty information of the important candidate training points. The global impact of selecting the training point is considered to ensure that the best training point is selected. The proposed method has been evaluated on three numerical problems and one practical engineering problem. The results show that the proposed method can construct a Kriging surrogate model for reliability analysis more efficiently while maintaining desired accuracy. The proposed method outperforms the other state-of-the-art methods in both accuracy and efficiency in the cases investigated. The proposed active learning function can be easily extended to integrate with different simulation methods to tackle extremely rare event problems in future research. In addition, it has the potential of being used to efficiently quantify the risks of real-world projects more comprehensive engineering modeling, and also for other reliability related problems, such as time-dependent reliability problems and reliability-based design optimization problems.

Acknowledgments

This research has been partly funded by the U.S. National Science Foundation (NSF) through awards CMMI-1762918 and 2000156. In addition, this work is supported in part by Lichtenstein endowment at The Ohio State University. These supports are greatly appreciated.

Reference

[1] Rubinstein RY, Kroese DP. Simulation and the Monte Carlo method. John Wiley & Sons; 2016.

[2] Au SK, Beck JL. Subset simulation and its application to seismic risk based on dynamic analysis. J Eng Mech 2003;129:901–17.

[3] Ditlevsen O, Madsen HO. Structural reliability methods. vol. 178. Wiley New York; 1996.

[4] Lemaire M. Structural reliability. John Wiley & Sons; 2013.

[5] Echard B, Gayton N, Lemaire M. AK-MCS: an active learning reliability method combining Kriging and Monte Carlo simulation. Struct Saf 2011;33:145–54.

[6] Blatman G, Sudret B. An adaptive algorithm to build up sparse polynomial chaos expansions for stochastic finite element analysis. Probabilistic Eng Mech 2010;25:183–97.

[7] Romero VJ, Swiler LP, Giunta AA. Construction of response surfaces based on progressive-lattice-sampling experimental designs with application to uncertainty propagation. Struct Saf 2004;26:201–19.
[8] Giunta AA, McFarland JM, Swiler LP, Eldred MS. The promise and peril of uncertainty quantification using response surface approximations. Struct Infrastruct Eng 2006;2:175–89.
[9] Zhao W, Fan F, Wang W. Non-linear partial least squares response surface method for structural reliability analysis. Reliab Eng Syst Saf 2017;161:69–77. https://doi.org/10.1016/j.ress.2017.01.004.
[10] Jones DR, Schonlau M, Welch WJ. Efficient Global Optimization of Expensive Black-Box Functions. J Glob Optim 1998;13:455–92. https://doi.org/10.1023/A:1008306431147.
[11] Bichon BJ, Eldred MS, Swiler LP, Mahadevan S, McFarland JM. Efficient global reliability analysis for nonlinear implicit performance functions. AIAA J 2008;46:2459–68.
[12] Lv Z, Lu Z, Wang P. A new learning function for Kriging and its applications to solve reliability problems in engineering. Comput Math Appl 2015;70:1182–97. https://doi.org/10.1016/j.camwa.2015.07.004.
[13] Yang X, Cheng X, Liu Z, Wang T. A novel active learning method for profust reliability analysis based on the Kriging model. Eng Comput 2021. https://doi.org/10.1007/s00366-021-01447-y.
[14] Sun Z, Wang J, Li R, Tong C. LIF: A new Kriging based learning function and its application to structural reliability analysis. Reliab Eng Syst Saf 2017;157:152–65.
[15] Wang Z, Shafieezadeh A. ESC: an efficient error-based stopping criterion for kriging-based reliability analysis methods. Struct Multidiscip Optim 2018. https://doi.org/10.1007/s00158-018-2150-9.
[16] Chen Z, Peng S, Li X, Qiu H, Xiong H, Gao L, et al. An important boundary sampling method for reliability-based design optimization using kriging model. Struct Multidiscip Optim 2015;52:55–70. https://doi.org/10.1007/s00158-014-1173-0.
[17] Moustapha M, Sudret B, Bourinet J-M, Guillaume B. Quantile-based optimization under uncertainties using adaptive Kriging surrogate models. Struct Multidiscip Optim 2016;54:1403–21. https://doi.org/10.1007/s00158-016-1504-4.
[18] Li G, Yang H, Zhao G. A new efficient decoupled reliability-based design optimization method with quantiles. Struct Multidiscip Optim 2020;61:635–47. https://doi.org/10.1007/s00158-019-02384-7.
[19] Zhang C, Shafieezadeh A. A quantile-based sequential approach to reliability-based design optimization via error-controlled adaptive Kriging with independent constraint boundary sampling. Struct Multidiscip Optim 2021. https://doi.org/10.1007/s00158-020-02798-8.
[20] Zhang C, Wang Z, Shafieezadeh A. Value of Information Analysis via Active Learning and Knowledge Sharing in Error-Controlled Adaptive Kriging. IEEE Access 2020;8:51021–34. https://doi.org/10.1109/ACCESS.2020.2980228.
[21] Wang Z, Shafieezadeh A. Real-time high-fidelity reliability updating with equality information using adaptive Kriging. Reliab Eng Syst Saf 2020;195:106735. https://doi.org/10.1016/j.ress.2019.106735.
[22] Zhang C, Wang Z, Shafieezadeh A. Error Quantification and Control for Adaptive Kriging-Based Reliability Updating with Equality Information. Reliab Eng Syst Saf 2021;207:107323. https://doi.org/10.1016/j.ress.2020.107323.
[23] Song C, Wang Z, Shafieezadeh A, Xiao R. BUAK-AIS: Efficient Bayesian Updating with Active learning Kriging-based Adaptive Importance Sampling. Comput Methods Appl Mech Eng 2022;391:114578. https://doi.org/10.1016/j.cma.2022.114578.
[24] UQLab Kriging (Gaussian process modelling) manual. UQLab Framew Uncertain Quantif 2017. http://www.uqlab.com/userguidekriging (accessed May 13, 2017).
[25] UQLab - The Framework for Uncertainty Quantification. Uqlab n.d. https://www.uqlab.com (accessed May 29, 2022).
[26] Yi J, Wu F, Zhou Q, Cheng Y, Ling H, Liu J. An active-learning method based on multi-fidelity Kriging model for structural reliability analysis. Struct Multidiscip Optim 2020. https://doi.org/10.1007/s00158-020-02678-1.
[27] Jiang C, Qiu H, Gao L, Wang D, Yang Z, Chen L. Real-time estimation error-guided active learning Kriging method for time-dependent reliability analysis. Appl Math Model 2020;77:82–98. https://doi.org/10.1016/j.apm.2019.06.035.
[28] Zhang C, Song C, Shafieezadeh A. Adaptive reliability analysis for multi-fidelity models using a collective learning strategy. Struct Saf 2022;94:102141. https://doi.org/10.1016/j.strusafe.2021.102141.
[29] Chaudhuri A, Marques AN, Willcox KE. mfEGRA: Multifidelity Efficient Global Reliability Analysis. ArXiv191002497 Phys Stat 2020.
[30] Moustapha M, Marelli S, Sudret B. Active learning for structural reliability: Survey, general framework and benchmark. Struct Saf 2022;96:102174. https://doi.org/10.1016/j.strusafe.2021.102174.

[31] Song H, Choi KK, Lee I, Zhao L, Lamb D. Adaptive virtual support vector machine for reliability analysis of high-dimensional problems. Struct Multidiscip Optim 2013;47:479–91. https://doi.org/10.1007/s00158-012-0857-6.
[32] Youn BD, Choi KK, Du L. Enriched Performance Measure Approach for Reliability-Based Design Optimization. AIAA J 2005;43:874–84. https://doi.org/10.2514/1.6648.
[33] Schueremans L, Van Gemert D. Benefit of splines and neural networks in simulation based structural reliability analysis. Struct Saf 2005;27:246–61.
[34] Rajashekhar MR, Ellingwood BR. A new look at the response surface approach for reliability analysis. Struct Saf 1993;12:205–20.
[35] Gayton N, Bourinet JM, Lemaire M. CQ2RS: a new statistical approach to the response surface method for reliability analysis. Struct Saf 2003;25:99–121.
[36] Huang X, Chen J, Zhu H. Assessing small failure probabilities by AK–SS: an active learning method combining Kriging and subset simulation. Struct Saf 2016;59:86–95.
[37] Bourinet J-M. Rare-event probability estimation with adaptive support vector regression surrogates. Reliab Eng Syst Saf 2016;150:210–21.
[38] Dundulis G, Žutautaitė I, Janulionis R, Ušpuras E, Rimkevičius S, Eid M. Integrated failure probability estimation based on structural integrity analysis and failure data: Natural gas pipeline case. Reliab Eng Syst Saf 2016;156:195–202. https://doi.org/10.1016/j.ress.2016.08.003.
[39] Janulionis R, Dundulis G, Grybėnas A, Kriūkienė R, Rimkevicius S. Degradation mechanisms and evaluation of failure of gas pipelines. Mechanics 2015;21:352–60. https://doi.org/10.5755/j01.mech.21.5.10196.
[40] Gas Pipeline Incidents: 9th Report of the European Gas Pipeline Incident Data Group (period 1970 - 2013) | Resolution Copper Project and Land Exchange Environmental Impact Statement n.d. https://www.resolutionmineeis.us/documents/egig-2015 (accessed June 12, 2022).
[41] Wang Y-L, Li C-M, Chang R-R, Huang H-R. State evaluation of a corroded pipeline. J Mar Eng Technol 2016;15.
[42] Arumugam T, Karuppanan S, Ovinis M. Finite element analyses of corroded pipeline with single defect subjected to internal pressure and axial compressive stress. Mar Struct 2020;72:102746. https://doi.org/10.1016/j.marstruc.2020.102746.
[43] Zheng T, Liang Z, Zhang L, Tang S, Cui Z. Safety assessment of buried natural gas pipelines with corrosion defects under the ground settlement. Eng Fail Anal 2021;129:105663. https://doi.org/10.1016/j.engfailanal.2021.105663.